DESIGNING FOR FREQUENCY AND TIME METROLOGY AT THE 10^{-18} LEVEL[*]

F. L. Walls, L. M. Nelson, and G. R. Valdez
Time and Frequency Division
National Institute of Standards and Technology
Boulder, CO 80303

Abstract

This paper examines some of the key parameters that significantly affect the overall architecture of a system that is being designed to measure frequency or time accuracy to 3×10^{-18}. Specifically, we investigate the timing errors in signal transmission for distances up to 100 m, the effect of changes in temperature and rf amplitude on timing (or frequency) errors in several available phase detectors, and the influence of measurement algorithms on the allowable level of white phase noise in the system as a function of the carrier frequency.

frequency stability; phase noise; timing errors; timing stability

Introduction

Several new frequency standards have been proposed that show a potential for a short-term frequency stability of order $2 \times 10^{-15}\tau^{-\frac{1}{2}}$ [1-4]. To measure the systematic shifts as a function of operating parameters and to measure the performance of these new clocks, it is desirable to have a measurement system that reaches the clock performance at a measurement time no longer than 10^4 s. Attaining this requires a resolution of approximately $\sigma_y(\tau) = 2 \times 10^{-17}$ at a measurement time of 10^4 s, or a timing error of 0.2 ps. Figure 1 shows the primary elements in such a measurement system.
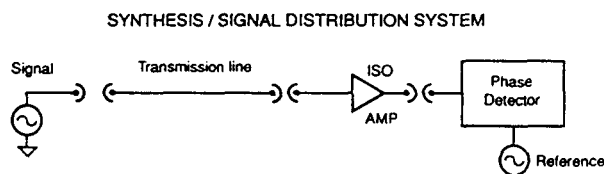
SYNTHESIS / SIGNAL DISTRIBUTION SYSTEM

Fig. 1 Overall block diagram showing the key elements for measuring the frequency or time of a remote clock.

In this paper we investigate the timing errors in signal transmission for distances up to 100 m, the effect of changes in temperature and rf amplitude on timing (or frequency) errors in several available phase detectors, and the influence of measurement algorithms on the allowable white phase noise in the system as a function of the carrier frequency.

Timing Errors in Signal Transmission

Potentially serious timing errors can be caused by the variation of transit time delay and the phase of the standing waves on the transmission line connecting the signal (clock) to the measurement system. The transit time delay of a signal is given by the length divided by the velocity of propagation. Signals transmitted to the measurement system and reflected from the load and then from the signal source lead to phase change of the signal at the load. Changes in the voltage standing wave ratio (VSWR) therefore lead to changes in the timing errors. The complete timing error from the transmission is

$$\delta t = L/(\beta c) + \rho_\ell \rho_s \sin\phi/(4\eta v_0) \qquad (1)$$

where L is the equivalent free-space length of the transmission line, c is the speed of light, β is the propagation factor, v_0 is the carrier frequency, η is the round trip attenuation, ρ_ℓ is the voltage reflection ratio from the load, ρ_s is the voltage reflection ratio from the source ($\rho = (VSWR - 1)/(VSWR + 1)$), and ϕ is the angle of the twice-reflected wave at the load relative to the primary signal. This equation assumes that the next order of reflected waves can be ignored ($\rho_s\rho_\ell/\eta \ll 1$). The first term is independent of frequency while the second term scales as $1/v_0$.

The variation in the timing error due to changes in $L/(\beta c)$ is potentially quite large for long transmission cables. Typical variations for several types of semi-rigid coaxial cables versus temperature are shown in Fig. 2 [5]. Typical insertion losses are of the order 1 dB/30 m at 5 MHz and 3 dB/30 m at 100 MHz for a 0.358 cm diameter cable. Cables with solid Teflon dielectric (Curve A) exhibit large hysteresis (due to the mismatch between the thermal expansion coefficient between the dielectric and the conductors) for temperature variations from 10°C to 20°C. Various attempts have been made to produce cable with a smaller temperature sensitivity by reducing the amount of Teflon dielectric or incorporating compensating materials (See Curves B-E of Fig. 2). Curve F of Fig. 2 shows the temperature sensitivity of a cable that uses SiO_2 powder as the dielectric. The phase variation from 18.3°C to 23.8°C is less than ± 0.5 ps over 30 m, while the insertion loss is 3.2 dB/30 m at 100 MHz. This generally satisfies the timing requirements for distances up to about 100 m. The primary disadvantage of this cable is the cost. Except in cases where there are large temperature variations,

one of the other cables from Fig. 2 usually performs acceptably at less cost for distances up to approximately 3 m. These data are summarized in Table 1.

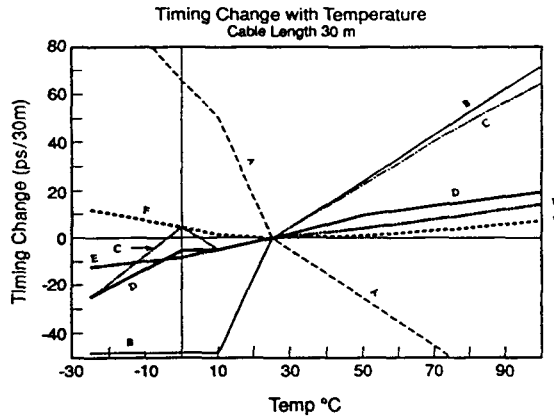

Timing Change with Temperature
Cable Length 30 m

Fig. 2 Timing error versus temperature for several different semi-rigid coaxial cables. Curve A, typical 0.358 cm (0.141") solid Teflon dielectric cable. Curve B, data for 0.483 cm (0.190") low density Teflon cable from W. L. Gore. Curve C, data for 0.358 cm cable with low density Teflon cable from Precision Tube. Curve D, data for 0.358 cm air-articulated cable from Precision Tube. Curve E, phase shift data for 0.358 cm ISOCORE cable from Rogers with the temperature coefficient of the dielectric matched to the conductors. Curve F data for 0.358 cm cable with SiO_2 dielectric from Kaman Instruments [5].

At 5 MHz, $1/(4 \, \nu_o)$ is 50 ns and numbers for ρ_ℓ and ρ_s are typically 1/3 (VSWR = 2). Such numbers can lead to large variations of timing error since VSWR is often dependent on temperature, rf drive level, and even supply voltage. Timing errors due to VSWR can be significantly improved by making ρ_ℓ, ρ_s, and sin ϕ small. At 5 MHz, for example, the timing error due to VSWR can be reduced below 11 ps by reducing VSWR below 1.1 at the source and load, and reducing sin ϕ below 0.1. At 100 MHz this term can be made less than 1 ps by making VSWR < 1.1 and sin ϕ < 0.1. The characteristic impedance of coaxial cables changes slightly from one batch to another, which might require a small adjustment in source and load impedances for the most critical applications.

An alternative approach to the problem is to use two-wa transmission measurements to correct for variations in th transmission medium. This technique has been pursued at th Jet Propulsion Laboratory where researchers hav concentrated on AM modulation of a laser transmitted ove fiber optic cables to solve both the attenuation of the sign; and timing errors for cable lengths up to 25 km. Their result [6], shown in Fig. 3, are very impressive. Although thi system is relatively costly, it is currently the only practic; approach for long transmission distances due to the proble; of attenuation.

Comparison of Measurement Algorithms

The minimum signal-to-noise ratio (S/N) that is consiste with the goals is set by the measurement algorithm and th time available to average the data. High precisic measurement systems are generally dominated by white pha: noise in the short-term, flicker phase, and environmental] driven offsets in the medium term, and bounded processes i the long term. If $\sigma_y(\tau)$ is used as the measure of frequenc stability, the observed stability depends on the level of whi phase noise, the level of white frequency noise, tl measurement bandwidth, and the measurement time and do(not depend on the number of samples [7]. If $\text{mod}\sigma_y(\tau)$ is use as a measure of frequency stability, the observed frequenc stability also depends on the number of measuremen averaged together to obtain $\text{mod}\sigma_y(\tau)$ [7].

The added phase noise from single and double balanc(mixers is flicker phase noise (usually $S_\phi(f) = 10^{-14}/f$ in uni of rad^2/Hz) for a Fourier frequency, f, from 0.1 to 1 kHz ar white phase at a level dependent on the IF amplifier at high frequencies. Typical levels are $10^{-16.5}$ to $10^{-17.7}$ rad^2/Hz [8 The added phase noise at Fourier frequencies below 0.01 l is often dominated by systematic and environmental effe(which are discussed in later sections. Most practical cloc have white frequency noise far above that of the mixer.

Figure 4 shows the frequency stability as determined by $\sigma_y($ and $\text{mod} \, \sigma_y(\tau)$ as a function of measurement time, and carri frequency for $S_\phi(f) = 8 \times 10^{-30}\nu_0^2/f^2$ (white frequency) $+ 10^{-14}/f$ (flicker phase) $+ 4 \times 10^{-27}\nu_0^2$ (white phase) rad^2/l and a measurement bandwidth of 1 kHz [8]. The first ter

TABLE 1. Timing errors due to thermal variations in cable length

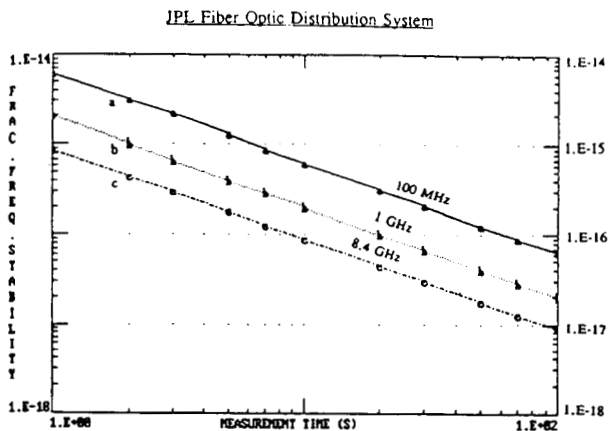| BASIC TYPES OF CABLES	Loss/30 m @ 100 MHz DIAMETER	σT/K 23-30°C	APPROXIMATE COST/30 m
SOLID DIELECTRIC PTFE common semi-rigid	3.4 dB 0.385 cm	1 ps/(30mK)	$ 210
MICROPOROUS W. L. GORE	2.8 dB 0.483.cm	1 ps/(30mK)	$4000
LOW DENSITY PTFE PRECISION TUBE	2.4 dB 0.385 cm	0.9 ps/(30mK)	$ 550
AIR ARTICULATED PTFE PRECISION TUBE	2.7 dB 0.385 cm	0.4 ps/(30mK)	$ 950
COMPENSATED DIELECTRIC ISOCORE ROGERS	3.5 dB 0.386 cm	0.18 ps/(30mK)	$ 657
SiO_2 DIELECTRIC KAMAN INSTRUMENTS	3.2 dB 0.385 cm	0.06 ps/(30mK)	$2200

Fig. 3 Fractional timing error versus measurement time (calculated from phase noise measurements) of the JPL fiber optic system for AM frequences of 100 MHz, 1 GHz, and 8.4 GHz. Timing error is $\tau\sigma_y(\tau)$. Adapted from [6]
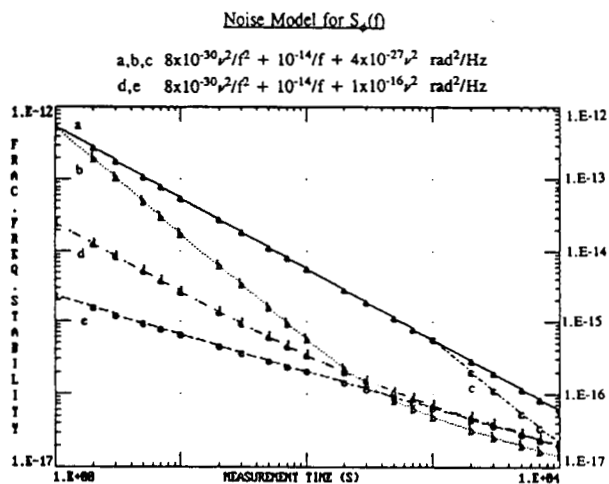

Fig. 4 Fractional frequency or timing error as a function of measurement time and measurement algorithm and input noise. Curves a, b, and c are for $S_\phi(f) = 8 \times 10^{-30}\nu^2/f^2 + 10^{-14}/f + 4 \times 10^{-27}\nu^2$ rad^2/Hz and a measurement bandwidth of 1 kHz. Curve a shows the results at 5 and 100 MHz using $\sigma_y(\tau)$ to calculate fractional stability. Curve b shows mod$\sigma_y(\tau)$ at 5 and 100 MHz for a minimum measurement time of 1 s, while curve c shows mod$\sigma_y(\tau)$ at 5 and 100 MHz for a minimum measurement time of 1000 s. Curve d shows $\sigma_y(\tau)$ at 5 MHz and Curve e shows $\sigma_y(\tau)$ at 100 MHz for $S_\phi(f) = 8 \times 10^{-30}\nu^2 + 10^{-14}/f + 10^{-16}$ rad^2/Hz.

originates from the assumed intrinsic frequency stability of the clock signal; the middle term originates from the mixer noise; and the last term is white phase noise assumed to originate in the clock or the measurement process. Also shown is the frequency stability at 5 MHz and 100 MHz when the white phase noise is equal to that of the mixer. Note that the frequency stability derived from mod$\sigma_y(\tau)$ is a function of the number of samples averaged to obtain mod$\sigma_y(\tau)$ when flicker phase and/or white phase noise dominates.

This example demonstrates that it is possible to achieve the desired time domain frequency stability even for relatively large levels of white phase noise, measurement times larger than 1000 s, and measurement bandwidths less than 1 kHz at either 5 or 100 MHz, assuming that the medium term noise from the measurement system is small enough. Furthermore, the use of multiple samples to compute the time of a clock reduces the timing error roughly as $n^{\frac{1}{2}}$ for white phase noise, $\ln(n)$ for flicker phase noise, and n for coherent signals, where n is the number of measurements averaged together to obtain the phase (time) of the clock signal [7,8]. The medium term noise is most often due to changes in temperature, rf drive levels, humidity, voltage, vibration and mechanical deformation, and pick-up of external signals.

Environmental Sensitivity of Phase Detectors

One measure of phase detector performance is the phase error $\delta\phi$ given by

$$\delta\phi = \delta V/k_d \qquad (2)$$

where δV is the dc output voltage error and k_d is the phase detection slope in V/rad [6]. For comparing different phase detector circuits as a function of carrier frequency, ν_o, it is more beneficial to use the timing error given by

$$\delta t = \delta V/(k_d 2\pi\nu_0) \quad s. \qquad (3)$$

The dc voltage error originates from imbalance between the I-V curves of the diodes, imbalance in the transformers, and asymmetric stray impedances. These imbalances are a function of the temperature and drive levels and therefore lead to changes in apparent phase or time with change in these parameters. The most important parameters that characterizes these effects are the isolation between the L and R ports, and the IF port. Table 2 shows approximate dc offsets as a function of L drive and isolation [9].

Table 2. DC offset voltage in mV for various combinations of LO drive level and isolation assuming a 50 Ω resistance on all ports [9].

LO DRIVE LEVEL – dBm

		0	+3	+7	+10	+13	+17	+20
	15	25.3	35.8	63.7	90.0	127.1	226.0	319.2
	20	14.2	20.1	35.8	50.6	71.5	127.1	179.5
	25	8.0	11.3	20.1	28.5	40.2	71.5	100.9
ISOLATION - dB	30	4.5	6.4	11.3	16.0	22.6	40.2	56.8
	35	2.5	3.6	6.4	9.0	12.7	22.6	31.9
	40	1.4	2.0	3.6	5.1	7.1	12.7	17.9
	45	0.80	1.1	2.0	2.9	4.0	7.1	10.1
	50	0.45	0.64	1.1	1.6	2.3	4.0	5.7

Figure 5 shows a typical circuit diagram for evaluating the phase detectors. The dc output (IF) port is terminated with the characteristic impedance which is typically 50 Ω for the double balanced mixers and 500 Ω for the single balanced mixer.
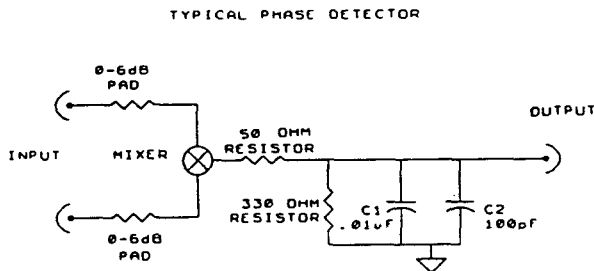
TYPICAL PHASE DETECTOR

Figure 5. Typical circuit diagram for evaluating the sensitivity of various phase detctors to variations in temperature and rf level.

Figures 6 to 8 show timing errors in selected phase detectors due to variation in input power and for two different temperatures for a carrier frequency of 5 MHz. One set of curves was taken without attenuators and the others with either 3 or 6 dB attenuators on the R and L inputs. At 5 MHz, the mixer with the individually matched diodes has a temperature coefficient of approximately 6 ps/°C when used with 6 dB pads, while the mixers with the 4 diodes on the same substrate exhibit a temperature coefficient of about 25 ps/°C. The sensitivity to power change is generally improved by adding 3 or 6 dB attenuators to the input ports. Without attenuators the power sensitivity is of order 1 ms/v_o per dB change in the power or 250 ps/dB at 5 MHz. The improvement due to the use of attenuators on the R and L inputs is thought to originate from the reduction in the cable VSWR generated by the phase detector load.
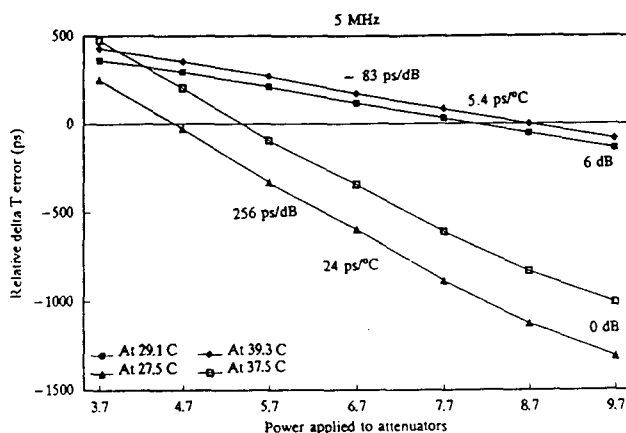
Figure 6. Timing errors in a double balanced mixer with individual diodes at a carrier frequency of 5 MHz as a function of drive power, input attenuators (0 dB and 6 dB), and temperature.
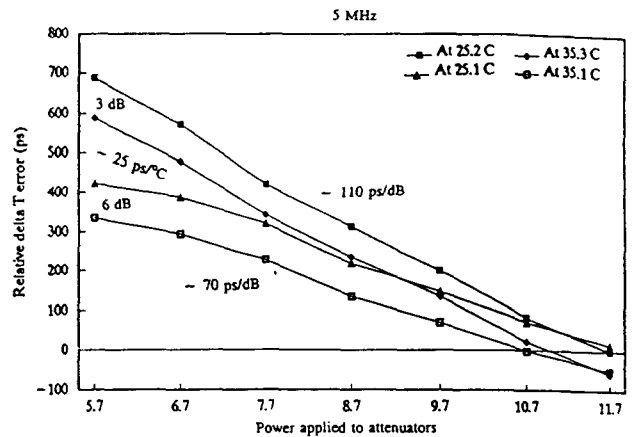
Figure 7. Timing errors in a double balanced mixer with a quad diode module, at a carrier frequency of 5 MHz as a function of drive power, input attenuators (3 dB and 6 dB), and temperature.
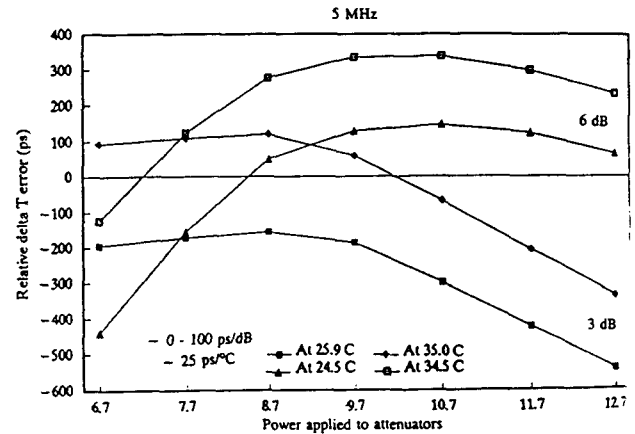
Figure 8. Timing errors in a single balanced mixer with : dual diode module, at a carrier frequency of 5 MHz as : function of drive power, input attenuators (3 dB and 6 dB) and temperature.

Figures 9 to 11 show the timing errors in selected phas detectors due to variations in input power and for tw different temperatures for a carrier frequency of 100 MHz One set of curves was taken without attenuators and the other were taken with either 3 or 6 dB attenuators on the R and ! inputs. The performance at 100 MHz of all three phas detectors versus temperature and power is improved over th results at 5 MHz by roughly the ratio of carrier frequencie: Temperature sensitivity is of the order 0.2 to 1 ps/°C. Th best temperature performance comes from the mixer wit individually matched diodes. The power sensitivity is of th order 0.1 to 1 ms/v_o per dB change in power or 1 to 10 ps/d at 100 MHz depending on mixer type, input power, an attenuation.

Discussion

It is much easier to achieve the desired time dom: performance of $\delta v/v_o = \delta t/t = 2 \times 10^{-17}$ at a measurem< time of 10^4 s for a carrier frequency of 100 MHz than fo MHz due to the sensitivity of presently available ph:
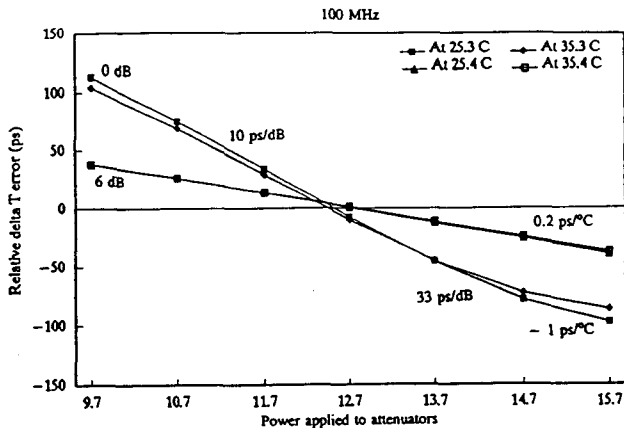
Figure 9. Timing errors in a double balanced mixer with a individual diodes, at a carrier frequency of 100 MHz as a function of drive power, input attenuators (0 dB and 6 dB), and temperature.
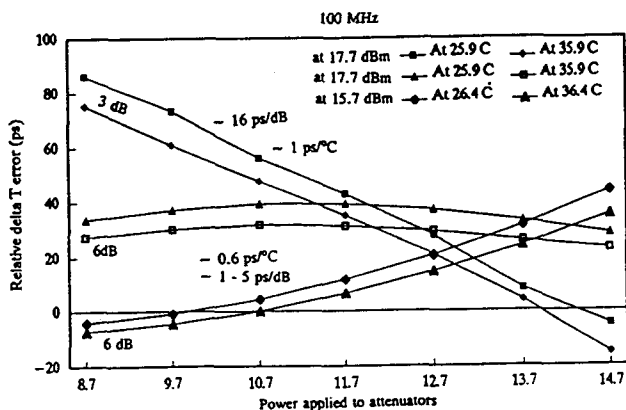

Figure 10. Timing errors in a double balanced mixer with a quad diode module, at a carrier frequency of 100 MHz as a function of drive power, input attenuators (3 dB and 6 dB), and temperature.
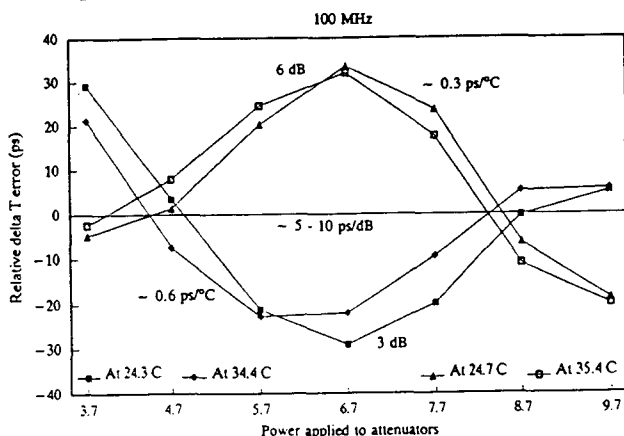

Figure 11. Timing errors in a single balanced mixer with a dual diode module, at a carrier frequency of 100 MHz as a function of drive power, input attenuators (3 dB and 6 dB), and temperature.

detectors to both temperature and rf amplitude. Even at 100 MHz it will probably be necessary to stabilize the temperature of the phase detectors to about 1°C and carefully match the characteristic impedance of the coaxial cable. For distances of up to 100 m, existing coaxial cables are probably sufficient. For longer distances we must consider either AM modulation of a laser transmitted over fiber optic cables or lower frequencies where the attenuation losses are smaller. The fiber optic system has already demonstrated excellent performance for distances up to 25 km and is probably the best choice. Going to 5 MHz would require two-way timing measurements to correct for the time dispersion in the transmission medium, much more effort to stabilize the operating parameters of the phase detector, and lowering the effects of VSWR at the source and the load.

ACKNOWLEDGEMENTS

References

1. D. J. Wineland, J. C. Bergquist, J. J. Bollinger, W. M. Itano, D. J. Heinzen, S. L. Gilbert, C. H. Manney, and M. G. Raizen, "Progress at NIST toward absolute frequency standards using stored ions," IEEE Trans. on Ultrasonics, Ferroelectrics, and Frequency Control, 37, 515-523 (1990).

2. J. D. Prestage, G. J. Dick, and L. Maleki, "Linear ion trap based atomic frequency standard," Proc. of 44th Ann. Frequency Control Symp., 1990, pp. 82-88.

3. S. Chu, "Laser manipulation of atoms and particles," Science, 253, 861-866 (1991).

4. J. L. Hall, M. Zhu, and P. Buch, "Prospects for using laser-prepared atomic fountains for optical frequency standards applications," J. Opt. Soc. Am. B, 6, 2194-2205 (1989).

5. Certain commercial equipment, instruments, or materials are identified in this paper in order to adequately specify the experimental procedure. Such identification does not imply recommendation or endorsement by the National Institute of Standards & Technology, nor does it imply that the materials or equipment identified are necessarily the best available for the purpose.

6. G. F. Lutes and R. T. Logan, "Status of frequency and timing reference signal transmission by fiber optics," Proc 45th Ann Frequency Control Symp., 1991, pp. 679-686.

7. "Characterization of clocks and oscillators," Eds. D. B. Sullivan, D. W. Allan, D. A. Howe, and F. L. Walls, NIST Tech Note 1337, 1990.

8. $\sigma_y(\tau)$ and mod$\sigma_y(\tau)$ were calculated using the SIGINT software package described in NISTIR 89-3916R. See also "Time domain frequency stability calculated from the frequency domain," Proc. of 4th European Frequency and Time Forum, 1990, pp. 197-204.

9. "Mixers as phase detectors," from 1985 Watkins-Johnson Catalog, pp. 666-673, 1985.